Structural Basis of Compound Recognition by Adenosine Deaminase

Takayoshi Kinoshita,*[,‡,§] Isao Nakanishi,[‡,||] Tadashi Terasaka,[⊥] Masako Kuno,[@] Nobuo Seki,[‡] Masaichi Warizaya,[‡] Hiroyoshi Matsumura,[#] Tsuyoshi Inoue,[#] Kazuhumi Takano,[+] Hiroaki Adachi,[×] Yusuke Mori,[×] and Takashi Fujii[‡]

Exploratory Research Laboratories, Fujisawa Pharmaceutical Company, Ltd., 5-2-3, Tokodai, Tsukuba, Ibaraki 300-2698, Japan, Medicinal Chemistry Research Laboratories and Medicinal Biology Research Laboratories, Fujisawa Pharmaceutical Company, Ltd., 2-1-6, Kashima, Yodogawa-ku, Osaka 532-8514, Japan, and Department of Materials Chemistry, Department of Material and Life Science, and Department of Electrical Engineering, Osaka University, 2-1 Yamadaoka, Suita, Osaka 565-0871, Japan

Received March 23, 2005; Revised Manuscript Received June 5, 2005

ABSTRACT: Structural snapshots corresponding to various states enable elucidation of the molecular recognition mechanism of enzymes. Adenosine deaminase has two distinct conformations, an open form and a closed form, although it has so far been unclear what factors influence adaptation of the alternative conformations. Herein, we have determined the first nonligated structure as an initial state, which was the open form, and have thereby rationally deduced the molecular recognition mechanism. Inspection of the active site in the nonligated and ligated states indicated that occupancy at one of the water-binding positions in the nonligated state was highly significant in determining alternate conformations. When this position is empty, subsequent movement of Phe65 toward the space induces the closed form. On the other hand, while occupied, the overall conformation remains in the open form. This structural understanding should greatly assist structure-oriented drug design and enable control of the enzymatic activity.

Vital homeostasis is precisely controlled by various proteins through numerous signal transduction systems and enzymatic reactions. Since the reactions of many proteins are accompanied by dynamic structural changes, structural monitoring of the snapshot structures during a reaction could lead to an improved understanding of this vital phenomenon and could lead to improved control of abnormal protein activity, which can cause serious disease. Understanding the nonligated structure as an initial state, as well as structures of complexes with substrate, cofactors, and/or various inhibitors, would be significant in elucidating the mechanism and may lead to new ideas on how enzyme activity is controlled and/or regulated. Multiple snapshots for enzymes such as human aldose reductase, porcine pancreatic elastase, and human p38 MAP kinase have been shown to be important in understanding the potency of inhibitors (*1*−*3*).

Adenosine deaminase (ADA)[1] has two distinct conformations, named the open form (Figure 1a,c) and the closed form (Figure 1b,d), and they were observed during examination of the ligated states with various inhibitors. The active site in the closed form consists of hydrophilic S0 and hydrophobic F0 subsites. It is believed that substrate adenosine (Figure 2) mainly binds to the S0 subsite, and the 2′- and 3′-hydroxyl groups of the ribose moiety bind in the F0 subsite (*4*). The hydroxyl groups of the ribose are seen from the solvent region side, and a water molecule exists in the F0 subsite. The S0 subsite is perfectly enclosed by a structural gate consisting of the peptide backbone of a β-strand (Leu182−Asp185) and two leucine side chains from an α-helix (Thr57−Ala73). In the open form, the gate is open. The open form strictly conserves the closed-form area consisting of the S0 and F0 subsites, and contains additional hydrophobic subsites defined as F1 and F2 around the gate (Figure 1d). Interestingly, both conformations are observed in the same crystal packing systems (*5*, *6*). Therefore, the structural difference is not an artifact due to crystal packing, but is a result of inhibitor-induced conformational change. However, the fundamental factors influencing conformational selectivity were unclear, even though many structures, except for the nonligated state, have been reported. For example, the inhibitor FR221647 (Figure 2) was produced through a de novo design procedure on the basis of the closed form (*7*), and in the crystal structure, FR221647 bound in the closed-form region, as expected. However, the protein conformation in the FR221647 complex is the open form, and no part of the inhibitor binds in the F1 and F2 regions. We had no clear explanation for this phenomenon at this point, although our design strategy using the closed form

* To whom correspondence should be addressed. E-mail: kinotk@b.s.osakafu-u.ac.jp. Phone: +81-72-2549819. Fax: +81-72-2549935.

‡ Exploratory Research Laboratories, Fujisawa Pharmaceutical Co., Ltd.

§ Current address: Department of Biological Science, Graduate School of Science, Osaka Prefecture University, 1-1, Gakuencho, Sakai, Osaka 599-8531, Japan.

|| Current address: Department of Theoretical Drug Design, Graduate School of Pharmaceutical Sciences, Kyoto University, Sakyo-ku, Kyoto 606-8501, Japan.

⊥ Medicinal Chemistry Research Laboratories, Fujisawa Pharmaceutical Co., Ltd.

@ Medicinal Biology Research Laboratories, Fujisawa Pharmaceutical Co., Ltd.

Department of Materials Chemistry, Osaka University.

+ Department of Material and Life Science, Osaka University.

× Department of Electrical Engineering, Osaka University.

[1] Abbreviations: ADA, adenosine deaminase; CD26, cluster of differentiation 26; EHNA, *erythro*-(+)-9-(2-hydroxy-3-nonyl)adenine; HDPR, 6-hydroxyl-1,6-dihydroxypurine riboside; MAP kinase, mitogen-activated protein kinase; SBDD, structure-based drug design.

10.1021/bi050529e CCC: $30.25 © 2005 American Chemical Society
Published on Web 07/15/2005

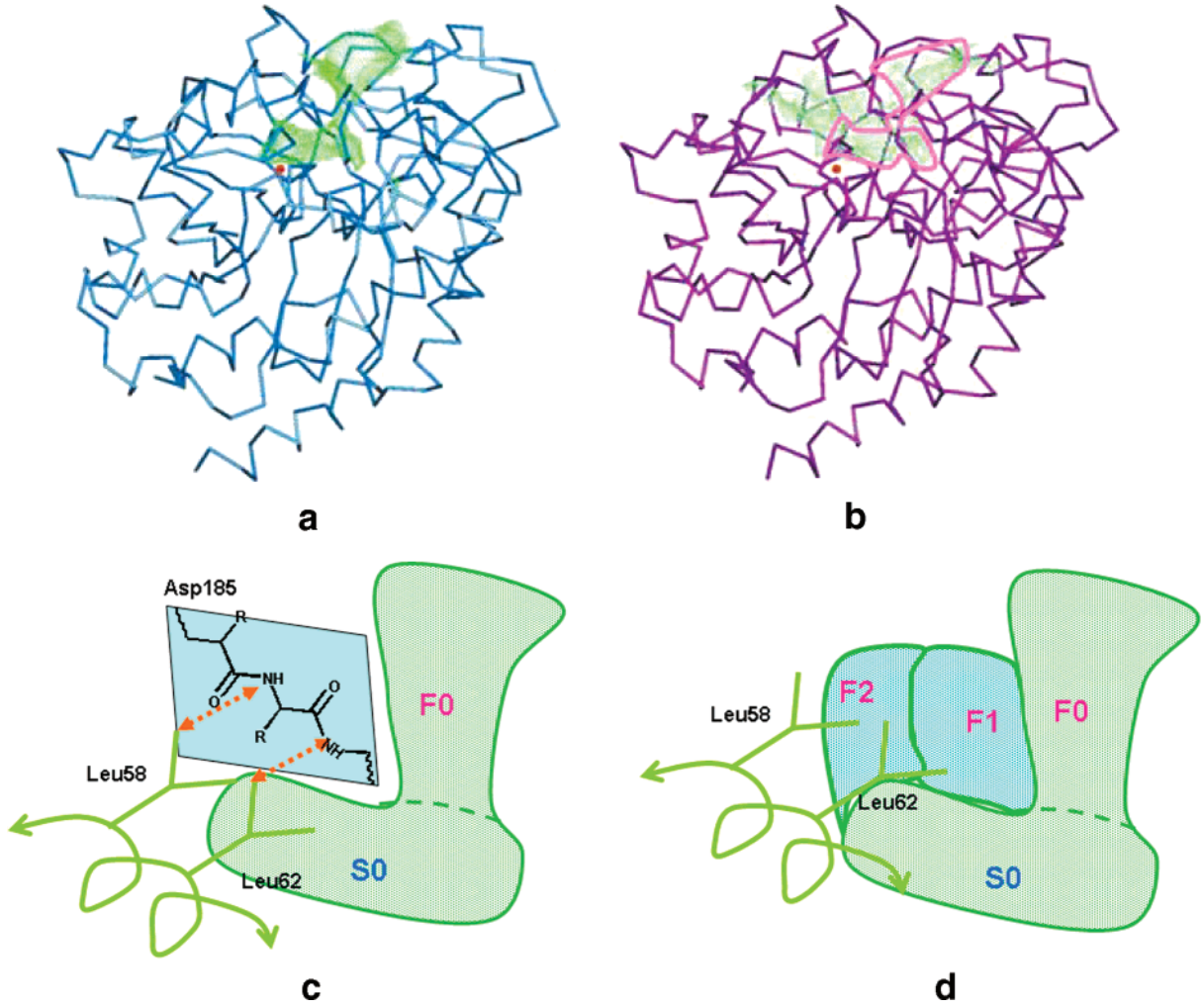

FIGURE 1: Closed and open forms. Zinc atoms in both forms are shown as red spheres. (a) Overall structure and active site envelope of the closed form. (b) Overall structure and active site envelope of the open form. The shape of the respective envelope is quite different, although overall both structures are similar. The outline of the envelope of the closed form (bold pink line) is superimposed on the open form. (c) A diagram of the active site envelope of the closed form, which consists of the hydrophilic S0 subsite and the hydrophobic F0 subsite. A structural gate above the S0 subsite, which consists of the peptide backbone of a β-strand (Leu182−Asp185) and two leucine residues from an α-helix (Thr57−Ala73), is closed. (d) Diagram of the active site envelope of the open form, which consists of the closed-form area and additional hydrophobic subsites F1 and F2. Additional subsites emerge due to movement of the α-helix.

was correct. In addition, it was further confirmed that all complexes had the open form through subsequent modification of FR221647 to other derivatives (*5*, *8*, *9*).

Biologically, adenosine deaminase is an essential enzyme for vital homeostasis in regulating the total amount of adenosine. Intracellular adenosine is involved in cellular energy production and purine metabolism, whereas extracellular adenosine acts as a signal messenger via specific cell surface receptors, exerting multiple physiologic actions in a variety of systems, including the immune system (*10*−*13*). Recently, adenosine has come to be considered an important factor in the attenuation of inflammation (*14*). Furthermore, it is also believed that extracellular ADA has an extra enzymatic function via binding with CD26 on the surface of activated lymphocytes (*15*). It is thus considered that an ADA inhibitor may change the concentration of adenosine specifically at inflamed sites and have potential as an anti-inflammatory drug with few side effects. A number of ADA inhibitors have been reported to date, for example, *erythro*-(+)-9-(2-hydroxy-3-nonyl)adenine [(+)-EHNA] and pentostatin (*16*, *17*). However, all have many problems, such as poor pharmacokinetics (*18*, *19*) and/or severe toxicity (*20*). We recently discovered a potent inhibitor with in vivo efficacy in models of inflammation and lymphoma (*8*, *9*).

For the next design step, including the major structural modification of inhibitors, it is critical to have a better comprehension of the molecular recognition mechanism. However, we did not know whether ADA would have alternative conformations. The nonligated conformation as an initial state would be a critical key for structural understanding. Very recently, we prepared high-quality crystals of nonligated ADA using a unique procedure involving the microstirring method of Adachi et al. (*21*), even though other methods have not been successful. As a result, we can now rationally predict the ADA recognition mechanism for various compounds on the basis of inspection of the active site using five snapshot structures, including a high-resolution crystal structure of the nonligated ADA as the initial state.

EXPERIMENTAL PROCEDURES

X-ray Crystallography. ADA from bovine intestine was purchased from Roche Diagnostics Inc. The crystals of the

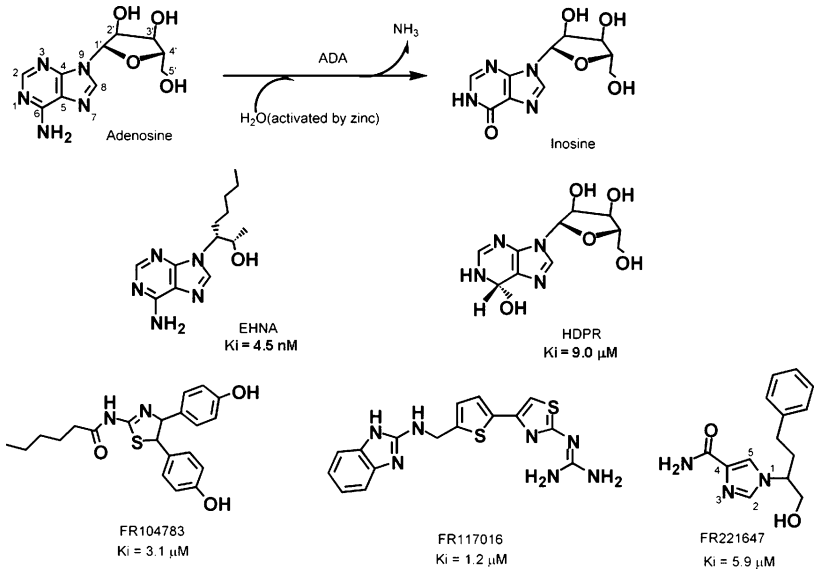

FIGURE 2: Chemical structures of ADA-related compounds. All compounds are drawn corresponding to the binding direction on the envelopes in Figure 1.

Table 1: Data Collection and Refinement Statistics[a]

	nonligated	FR104783
data collection		
space group	$P4_32_12$	$P4_32_12$
unit cell dimensions (Å)	$a = 73.73$, $c = 134.01$	$a = 76.87$, $c = 134.13$
no. of observations	136036	67844
no. of unique reflections	34175	14524
completeness (%)	97.5 (97.2)	99.3 (99.9)
R_{merge} (%)[b]	5.9 (32.2)	10.2 (36.7)
I/σ	22.3 (2.5)	8.2 (2.1)
refinement statistics		
resolution (Å)	28.43−1.80	29.15−2.50
no. of reflections	33895	14422
total no. of atoms	3036	3069
R-factor (%)	23.0	26.4
R_{free} (%)	26.7	26.8
rms deviation		
bond lengths (Å)	0.005	0.024
bond angles (deg)	1.2	3.9

[a] Values in parentheses are for the highest-resolution shell. [b] $R_{merge} = \sum_h\sum_j|I_{hj} - \langle I_h\rangle|/\sum_h\sum_j|I_{hj}|$, where h represents a unique reflection and j represents symmetry-equivalent indices. I is the observed intensity, and $\langle I\rangle$ is the mean value of I.

apoenzyme and the FR104783 complex used for data collection were prepared as described in detail elsewhere (*6*, *22*). The crystals grew to maximum dimensions of approximately 0.3 mm × 0.2 mm × 0.2 mm in 2 weeks. All intensity data sets were collected at 100 K on a Rigaku R-AXIS V imaging-plate system at beamline BL24XU of the SPring-8 synchrotron facility. They were integrated and scaled with Crystal Clear (Rigaku, Tokyo, Japan). The structures were determined by the molecular replacement method using AMoRe (*23*) and the holoenzyme in the HDPR−ADA complex (*6*) or the FR117016−ADA complex (*5*) as a search probe. Quanta (Accelrys) was used for model building and CNX (Accelrys) for structure refinement. Data collection and refinement statistics of both structures are given in Table 1. In all complexes, two amino acids from the N-terminus and five from the C-terminus were omitted from the final model because of ambiguous or discontinuous electron density for the corresponding regions. Superposition studies of the free state against the respective complexes were performed with Quanta (Accelrys).

Enzyme Assay. Human recombinant ADA was expressed and purified from an ADA-deficient bacterial strain (*4*). The reaction velocity (v) was measured by following the change in absorbance at 265 nm (A_{265}) resulting from the deamination of adenosine. Reaction mixtures in a total volume of 200 μL contained 25 milliunit of ADA/mL and varying concentrations of adenosine and test compounds in 10 mM phosphate-buffered saline (pH 7.4). The reaction was started by addition of ADA to a mixture of adenosine and test compound. The reaction was followed at room temperature by recording the decrease in A_{265} for 5 min using a SPECTRAmax 250 apparatus (Molecular Devices) to automatically calculate V_{max}. The inhibition constant (K_i) values of test compounds were determined using a Dixon plot.

Coordinates. Coordinates and structure factors have been deposited with the Protein Data Bank (entries 1VFL and 1WXY for nonligated ADA and the FR104783 complex, respectively). Other coordinates used in this work were obtained from the PDB (entries 1KRM, 1NDV, and 1NDW for HDPR, FR117016, and FR221647 complexes, respectively).

RESULTS

Structural Analysis of Nonligated ADA and a FR104783−ADA Complex. Our first crystallization trials with nonligated ADA, performed in a manner similar to that for obtaining inhibitor−ADA complex crystals, failed, although the results of dynamic light scattering experiments suggested a high likelihood of crystallization, since the size distribution of the ADA molecules in the sample solution was narrow monomodal (*24*). Rescreening with a Crystal Screen HT screening kit (Hampton Research) also failed, even when optionally combined with procedures involving the presence of an agarose gel or a strong magnetic field, conditions employed for improving the quality of the inhibitor−ADA complex crystals (*25*). Very recently, we adopted the microstirring method (*21*), which resulted in high-quality crystals of the apoenzyme. The crystals diffracted up to 1.8 Å resolution, and finally, we could obtain the refined nonligated structure containing water molecules in the active site, allowing for a precise discussion.

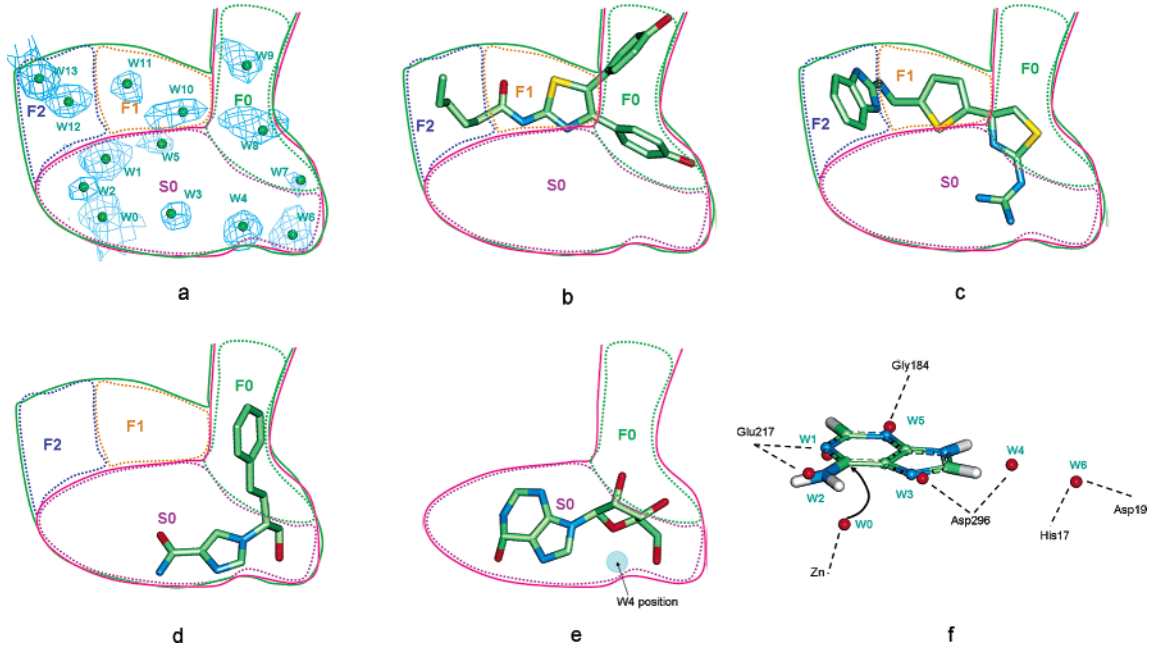

FIGURE 3: Active site diagrams of the nonligated and ligated structures. The closed and open forms are depicted as magenta and green lines, respectively. The open form embraces the closed-form area. Individual subsites are displayed as dotted lines. (a) Nonligated state. Fourteen water molecules (W0−W14) are bound to the respective subsites. (b) FR104783 complex. The inhibitor binds only with hydrophobic subsites and does not use the hydrophilic S0 subsite. (c) FR117016 complex. The inhibitor fully occupies the F1 and F2 subsites and partially occupies the F0 and S0 subsites. (d) FR221647 complex. The inhibitor binds using the F0 and S0 subsites and does not use the F1 and F2 subsites. (e) HDPR complex. The inhibitor fully occupies the S0 subsite and partially does the F0 subsite. (f) Hypothetical superimposition of an adenine ring onto the hydrophilic water molecules in the nonligated state. W1−W3 and W5 correspond to the nitrogen atoms.

On the other hand, crystals of the FR104783−ADA complex were easily obtained using the same procedure as the other ligated ADA structures (*6*). The crystals diffracted up to 2.5 Å resolution, and we could obtain a good refined structure.

The *R*-factor of both structures is somewhat high (Table 1), since several flexible side chains of residues exist on the surface, far from the active site. The surface of ADA interacts with the CD26 molecule, and several amino acids from the N-terminus and the C-terminus were omitted from the final model because of ambiguous or discontinuous electron density for the corresponding regions. However, the electron density maps around the active site, including water molecules, were sufficiently clear to guarantee the accuracy of the active site in the final models.

Structural Features of the Nonligated State. The overall structure of the nonligated state is the open form. Nonligated ADA crystallized in the same crystal form as other ligated ADA complexes. All crystals of nonligated and ligated ADA belong to the same space group, $P4_32_12$, and have similar crystallographic parameters. Therefore, careful comparison in the active site should afford key information for elucidating the molecular recognition mechanism.

Fourteen water molecules bind in the active site consisting of the S0, F0, F1, and F2 subsites (Figure 3a). A total of seven water molecules, W0−W6, bind in the S0 subsite. W0 coordinates to the active center of zinc with a 2.1 Å distance. Thus, it might be identical to the activated water molecule according to the previous report (*4*, *6*, *26*). The other six water molecules bind via hydrogen bonds. W1 and W2 interact with Glu217, which makes hydrogen bonds with two water molecules tethered by Glu186, Ser265, and Thr269. W3 and W4 interact with Asp296, which has no other interactions and has allowance for small movement. W5 interacts with the backbone NH group of Gly184. W6 interacts with Asp19 and His17. The imidazole of His17 is fixed because it is coordinated to zinc. W6 corresponds to the 5′-hydroxyl group of substrate ribose. Water molecules W1−W5 also form hydrogen bonds with each other and create a planar geometry. Thus, these water-binding positions are considered primed for binding the nitrogen atoms of the substrate adenine moiety based upon predictions based on the structure of the HDPR complex (Figure 3f). Besides W0−W6, seven weak-binding water molecules exist in the hydrophobic subsites: W7−W9 in the F0 subsite of the closed-form area, W10 and W11 in the F1 subsite, and W12 and W13 in the F2 subsite. *B*-factors in the range of 36−61 for these water molecules are higher than those for hydrogen-bonding waters W0−W6 (24−44), and the electron density envelopes for W7−W13 are broad.

Nonligated versus Ligated States of the Open Form. The nonligated structure, as well as ligated structures with various FR compounds, is the open form. Therefore, simple comparison of the active site should make clear the molecular recognition mechanism as far as the open form is concerned. The FR104783 molecule binds to the active site using only hydrophobic F0, F1, and F2 subsites and fully occupies these subsites (Figure 3b). The inhibitor completely displaces the water molecules from the hydrophobic environment. The aliphatic moiety and thiazole ring make hydrophobic interactions with both sides of the hydrophobic gate consisting of the F1 and F2 subsites. Two phenyl groups fully occupy the F0 subsite. Interestingly, the inhibitor binds far from the active center, does not bind to the hydrophilic S0 subsite at

Table 2: Atoms in the Respective Complex Corresponding to Water Molecules in the Nonligated State

nonligated	FR104783	FR117016	FR221647	HDPR
W0	H_2O	H_2O	H_2O	OH
W1	H_2O	H_2O	H_2O	N[e]
W2	H_2O	H_2O	H_2O	H[f]
W3	H_2O	N[a]	N[b]	N[g]
W3′	no space	H_2O	N[c]	no space
W4	H_2O	N[a]	C[d]	empty
W5	H_2O	H_2O	H_2O	N[h]
W6	H_2O	H_2O	OH	OH

[a] Nitrogen atoms of the guanidyl group. [b] N3 atom of the imidazole ring. [c] Nitrogen atom of the carbamoyl group. [d] C2 atom of the imidazole ring. [e] N1 atom. [f] Hydrogen atom bound to the C6 atom. [g] N7 atom. [h] N3 atom of the purine ring.

all, and makes no direct hydrogen bond with the protein. As a result, the complex exactly conserves all water molecules in the S0 subsite (Table 2).

The FR117016 molecule fully occupies the F1 and F2 subsites and partially occupies the F0 subsite (Figure 3c). The thiophene and benzimidazole rings are interposed by the hydrophobic gate consisting of the F1 and F2 subsites. The thiazole ring occupies one half of the F0 subsite, and the F0 subsite has extra space. The guanidyl group of the inhibitor binds to the S0 subsite, and six water molecules bind in the S0 subsite (Table 2). Waters W0, W1, W2, W5, and W6 are conserved. The W3 position moves forward to the direction of W2, and the W3′ position newly emerges between the W3 and W4 positions. A water molecule occupies the W3 position; two guanidyl nitrogen atoms occupy the W3′ and W4 positions, and the water and both nitrogen atoms make hydrogen bonds with Asp296.

The FR221647 molecule fully occupies most of the F0 hydrophobic subsite, but F1 and F2 subsites in the complex remain empty (Figure 3d). The inhibitor occupies approximately half of the S0 subsite, and five water molecules bind to the S0 subsite (Table 2). Waters W0, W1, W2, and W5 are conserved. A water molecule occupies the shifted W3 position, and imidazole N3 and C2 atoms of the inhibitor occupy the W3′ and W4 positions, respectively. Asp296 moves slightly and makes hydrogen bonds with the amino group and the N3 atom of the imidazole ring. Asp296 is flexible in the active site and thereby can adjust to keep the interaction with the respective inhibitor. The hydroxyl group of the inhibitor occupies the W6 position and forms hydrogen bonds with Asp19 and His17.

Hydrophobic interaction patterns vary, and the interaction is significant for molecular recognition. FR104783 has micromolar activity only due to the hydrophobic interaction contributions, with no hydrogen bonds. FR221647 uses only the F0 subsite, and water molecules remain in the F1 and F2 subsites in the complex. Derivatives of FR221647 directed forward to full occupation of the F1 and F2 subsites bound 800 times more tightly (*5*). Therefore, higher occupation of the hydrophobic subsites would presumably give higher activity. With regard to the hydrophilic S0 subsite, the water-binding positions of the nonligated state are important for molecular recognition. All positions are occupied, although the W3 and W4 positions are flexible due to the mobility of Asp296. As a result, all hydrogen acceptors and donors in the S0 subsite were replaced with heteroatoms of the respective inhibitor in forming the complexes.

Open Form versus Closed Form. HDPR eliminates all water molecules in the S0 subsite and fully occupies the S0 subsite (Figure 3e). The inhibitor induces a large conformational change from the open form as the initial state to the closed form. In the closed form, the α-helix (Thr57−Ala73) consisting of the structural gate slightly kinks at Phe65. As a result of this kink, two leucine residues, Leu58 and Leu62, in the α-helix move forward to the hydrophobic F1 and F2 subsites of the open form, and shut the structural gate. Leu58 moves ∼5 Å, although Cα movement at Phe65 is small (only ∼0.5 Å). Finally, the F1 and F2 subsites disappear during the conformational change to the closed form.

On the other hand, the closed form regions of both forms are structurally conserved (Figure 3). The hydrophobic F0 subsite has large allowance and no restrictions for molecular recognition. The W7−W9 water molecules in the nonligated state are fully replaced by two phenyl moieties in the FR104783 complex, partially by the thiazole ring in the FR117016 complex, by the methylene chain and the phenyl ring in the FR221647 complex, and slightly by two hydroxyl groups in the HDPR complex. With respect to the hydrophilic S0 subsite in common with the open form, any non-hydrogen atom occupies the W0−W6 positions and the number of hydrogen bonds is conserved. In the HDPR complex representing the closed form, what atoms occupy these positions? The W0 position is occupied by a hydroxyl group bound to the C6 atom, and the group coordinates to the active center zinc. The W1, W3, and W5 positions correspond to the N1, N7, and N3 atoms of the purine frame, respectively. The W6 position is occupied by the 5′-hydroxyl group of the ribose moiety. The W2 position is occupied by the hydrogen atom bound to the C6 atom. Therefore, it is assumed that the W2 position is ready for the leaving amine group of the substrate adenosine based upon the superimposition of the HDPR complex as a transition state mimic onto the nonligated structure as an initial state (Figure 3f). The W2 position in the HDPR complex is located ∼2 Å from the C6 atom in the same direction as the hydrogen atom, and is partially occupied by the hydrogen atom bound to the C6 atom. Thus, the hydrogen atom perhaps contributes to some part of the interaction with Glu217 in place of the leaving amine group in the transition state. Moreover, Glu217 is stabilized and fixed by two water molecules, which are not different from the highlighted water molecules. Surprisingly, the W4 position is empty in the closed form, although the position is occupied in the open form. One of the hydrogen bond acceptors of Asp296 remains free in the closed form without other supporting factors such as Glu217.

Occupancy of the W4 position should be most significant for large conformational changes. HDPR induces conformational change to the closed form, although the inhibitor can bind to the open form. FR221647 binds to the open form, although the inhibitor uses only the closed-form area. The F1 and F2 subsites are irrelevant to the mechanism of conformational alternation, because HDPR and FR221647 do not use these two subsites in the respective forms. Therefore, it appears that an important key in determining the mechanism is embraced in the closed-form area. In the F0 subsite, no common features were uncovered. The conformation around the F0 subsite is rigid even if a moiety binds to the subsite in the various complexes. The S0 subsite, which is important for substrate binding, has differences

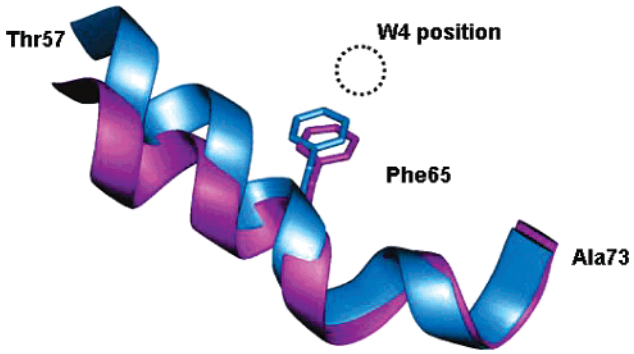

FIGURE 4: α-Helix (Thr57−Ala73) consisting of the structural gate of the active site. The helix of the open form (magenta ribbon) stays back when the W4 position is occupied by an atom. On the other hand, the helix of the closed form (blue ribbon) moves forward to the W4 position when the position is empty. The subsequent kink at Phe65 causes a change in the active site conformation.

between the closed and open forms. In the HDPR complex, the W4 position is located near the C8 atom of the purine ring with a distance of 2.6 Å, and the C2′ and C3′ atoms of the ribose moiety with distances of 2.5 and 2.4 Å, respectively. The hydrogen atoms bound to these carbon atoms directed to the W4 position. The crowded situation should induce elimination of the W4 water in HDPR binding, although an energy penalty arises due to free Asp296. The W4 position is also located near the Cζ atom of Phe65 with a distance of 3.5 Å in the nonligated state and a distance of 3.0 Å in the HDPR complex. Phe65 in the closed form is ∼0.5 Å closer to the W4 position (Figure 4). As a result, the side chain of Phe65 contributes to the interaction with a part of the adenine frame and the ribose moiety. Slight movement at the Phe65 residue results in a large conformational change in the closed form. Only in the case in which the position is empty can Phe65 move toward the W4 position. Subsequently, the α-helix kinks at Phe65, and finally, the kink leads to the closed from. In fact, when ADA is in the open form, the W4 position is always occupied: water for the nonligated form and the FR104783 complex, the guanidyl nitrogen atom for the FR117016 complex, and the imidazole carbon atom for the FR221647 complex.

Additional factors influencing the closed form may be van der Waals interactions with the surface of the S0 subsite, as well as the hydrophobic interaction at the closed gate. Phe65 also takes part in the interaction. In result of occupation at the water-binding sites in the S0 subsite, inhibitor or substrate should fill the S0 space. Thus, full occupation of the hydrophilic subsite causes interactions with the inner side of the S0 subsite, and these interactions bring about energy gain to some extent. Actually, all substrate analogues such as HDPR, which almost fully occupy the hydrophilic S0 subsite, induce the closed form. Furthermore, we observed that introduction of the methyl group into the S0 subsite leads to an ∼30 times higher binding affinity, but the same introduction into the F2 subsite yields little activity (*8*, *9*). Furthermore, in complexes with the closed form, the W4 position is empty (*4*, *6*, *26*).

DISCUSSION

We have herein achieved a comprehensive understanding of the conformational selection rule, regarding whether ADA exists in closed or open forms. Occupancy at only a single water-binding position in the nonligated state is critical for

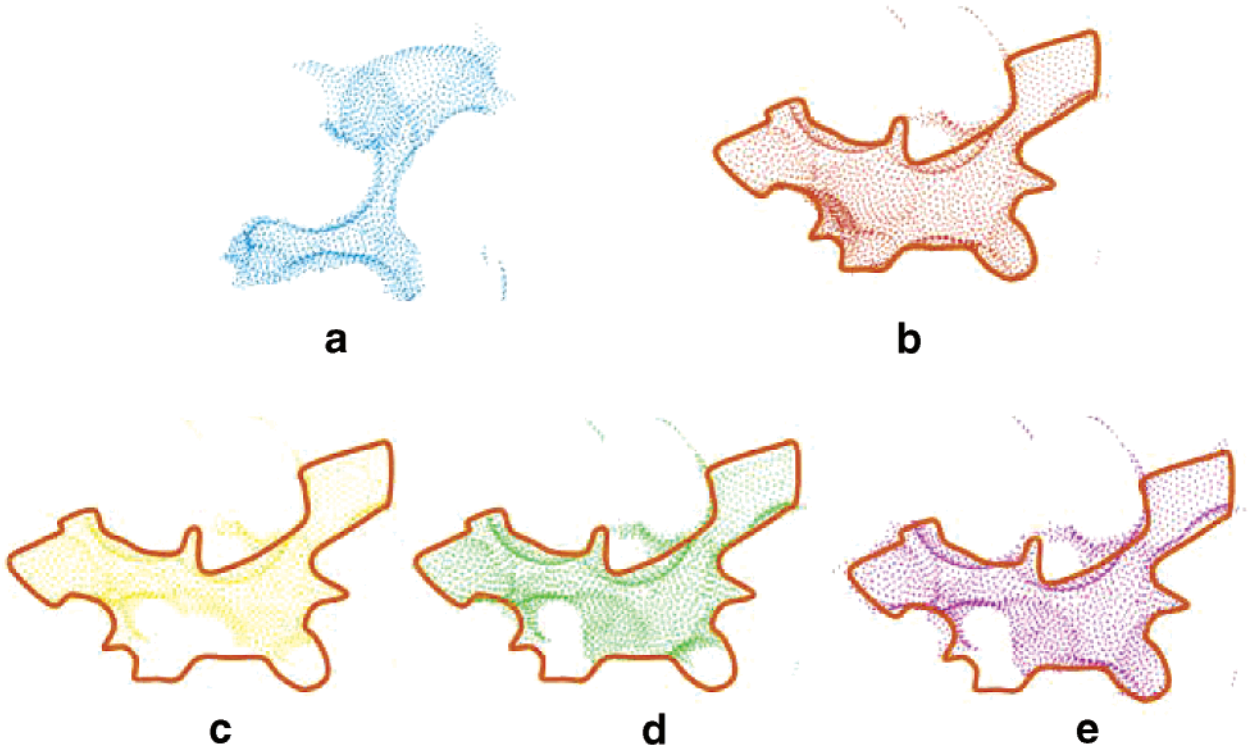

FIGURE 5: Various envelopes of active sites. (a) Envelope of the closed form. (b) Envelope of the open form. The outline of envelope b is superimposed on the respective open form. (c) Envelope calculated for the open form, leaving all water molecules in the S0 subsite (W0−W6). The binding contacts of FR104783 correspond to this envelope. (d) Envelope calculated for the open form leaving the W0−W2, W5, and W6 molecules. The binding contacts of FR117016 correspond to this envelope. (e) Envelope calculated for the open form leaving the W0−W2 and W5 molecules. The binding contacts of FR221647 correspond to this envelope.

switching conformations. Additional factors favoring the closed form are presumed to be the energy gains from van der Waals interactions with the surface of the S0 subsite.

Comprehension of these mechanisms should assist in structure-oriented drug design. As a first step, it is necessary that occupancy at the W4 position be considered. When the W4 position is empty, design can be done using the closed form, and the W0−W3, W5, and W6 positions should be occupied by heteroatoms. Moreover, the S0 subsite may be filled by the designed inhibitor.

On the other hand, when the W4 position is occupied, design can be performed using the open form. Additionally, many pseudo-open forms could be considered according to the variety in the number of waters remaining in the S0 subsite (Figure 5). It is probably important that some of these waters remain during structure-based drug design since heteroatoms may not be able to replace them. Removal of hydrogen-bonding or coordinating waters generally causes a large energy penalty, if the hydrogen bond contribution to binding is not offset. The three FR compounds have practically similar activities, although the number of residual water molecules is different in the respective complexes. All seven water molecules remain in the FR104783 complex, six water molecules in the FR117016 complex, and four water molecules in the FR221647 complex. Other combinations of remaining waters may also be considered.

The flexibility of the respective water-binding positions in the hydrophilic region is also significant for molecular recognition and drug design. The W0−W2 and W6 positions should be considered as rigid, since the residues tethering these water molecules are fixed by other factors. W0 binds to the zinc atom fixed by three histidine residues and one aspartic acid; W1 and W2 bind to Glu217 tethered by two fixed water molecules, and W6 binds to His17 fixed by the zinc atom. On the other hand, the W3−W5 positions should be considered as flexible, since the residues tethering these water molecules are free from any other atoms. Flexibility of Asp296 in front of the W3 and W4 positions is important for keeping the hydrogen bond with the substrate N7 atom, which may move in the enzymatic reaction.

We believe that this structural comprehension should lead to discovery of ADA inhibitors by structure-oriented drug design and by virtual screening, and that these concepts, including multiple active site envelopes, should be applicable to other proteins.

ACKNOWLEDGMENT

We are grateful to the SOSHO Project for the preparation of the nonligated state. We also thank Dr. David Barrett (Fujisawa Pharmaceutical Co., Ltd.) for valuable comments and help in the preparation of the manuscript.

REFERENCES

1. Kinoshita, T., Miyake, H., Fujii, T., Takakura, S., and Goto, T. (2002) The structure of human recombinant aldose reductase complexed with the potent inhibitor zenarestat, *Acta Crystallogr. D58*, 622−626.
2. Kinoshita, T., Nakanishi, I., Sato, A., and Tada, T. (2003) True interaction mode of porcine pancreatic elastase with FR136706, a potent peptidyl inhibitor, *Bioorg. Med. Chem. Lett. 13*, 21−24.
3. Wang, Z., Canagarajah, B. J., Boehm, J. C., Kassaisa, S., Cobb, M. H., Young, P. R., Abdel-Meguid, S., Adams, J. L., and Goldsmith, E. J. (1998) Structural basis of inhibitor selectivity in MAP kinases, *Structure 6*, 1117−1128.
4. Sideraki, V., Mohamedali, K. A., Wilson, D. K., Cheng, Z., Kellems, R. E., Quiocho, F. A., and Rudolph, F. B. (1996) Probing the functional role of two conserved active site aspartates in mouse adenosine deaminase, *Biochemistry 35*, 7862−7872.
5. Terasaka, T., Kinoshita, T., Kuno, M., and Nakanishi, I. (2004) A highly potent non-nucleoside adenosine deaminase inhibitor: Efficient drug discovery by intentional lead hybridization, *J. Am. Chem. Soc. 126*, 34−35.
6. Kinoshita, T., Nishio, N., Nakanishi, I., Sato, A., and Fujii, T. (2003) Structure of bovine adenosine deaminase complexed with 6-hydroxy-1,6-dihydropurine riboside, *Acta Crystallogr. D59*, 299−303.
7. Terasaka, T., Nakanishi, I., Nakamura, K., Eikyu, Y., Kinoshita, T., Nishio, N., Sato, A., Kuno, M., Seki, N., and Sakane, K. (2003) Structure-based de novo design of non-nucleoside adenosine deaminase inhibitors, *Bioorg. Med. Chem. Lett. 13*, 1115−1118.
8. Terasaka, T., Okumura, H., Tsuji, K., Kato, T., Nakanishi, I., Kinoshita, T., Kato, Y., Kuno, M., Seki, N., Naoe, Y., Inoue, T., Tanaka, K., and Nakamura, K. (2004) Structure-based design and synthesis of non-nucleoside, potent, and orally bioavailable adenosine deaminase inhibitors, *J. Med. Chem. 47*, 2728−2731.
9. Terasaka, T., Kinoshita, T., Kuno, M., Seki, N., Tanaka, K., and Nakanishi, I. (2004) Structure-Based Design, Synthesis, and Structure−Activity Relationship Studies of Novel Non-nucleoside Adenosine Deaminase Inhibitors, *J. Med. Chem. 47*, 3730−3743.
10. Ralevic, V., and Burnstock, G. (1998) Receptors for purines and pyrimidines, *Pharmacol. Rev. 50*, 536−543.
11. Olsson, R. A., and Pearson, J. D. (1990) Cardiovascular purinoceptors, *Physiol. Rev. 70*, 413−492.
12. Shryock, J. C., and Belardinelli, L. (1997) Adenosine and adenosine receptors in the cardiovascular system: Biochemistry, physiology, and pharmacology, *Am. J. Cardiol. 79*, 2−10.
13. Guieu, R., Dussol, B., Halimi, G., Bechis, G., Sampieri, F., Berland, Y., Sampol, J., Courand, F., and Rochat, H. (1998) Adenosine and the nervous system: Pharmacological data and therapeutic perspectives, *Gen. Pharmacol. 31*, 553−561.
14. Ohta, A., and Sitkovsky, M. (2001) Role of G-protein-coupled adenosine receptors in downregulation of inflammation and protection from tissue damage, *Nature 414*, 916−920.
15. Kamaoka, J., Tanaka, T., Nojima, Y., Schlossman, S. F., and Morimoto, C. (1993) Direct association of adenosine deaminase with T cell activation antigen, CD26, *Science 30*, 466−469.
16. Bessodes, M., Bastian, G., Abushanab, E., Panzica, R. P., Berman, S. F., Marcaccio, E. J., Chen, S. F., Stoeckler, J. D., and Parks, R. J. (1982) Effect of chirality in erythro-9-(2-hydroxy-3-nonyl) adenine (EHNA) on adenosine deaminase inhibition, *Biochem. Pharmacol. 31*, 879−882.
17. Agerwal, R. P., Spector, T., and Parks, R. E. (1977) Tight-binding inhibitors IV. Inhibition of adenosine deaminase by various inhibitors, *Biochem. Pharmacol. 26*, 359−367.
18. McConnell, W. R., El-Dareer, S. M., and Hill, D. L. (1980) Metabolism and disposition of erythro-9-(2-hydroxy-3-nonyl)[^{14}C]-adenine in the rhesus monkey, *Drug Metab. Dispos. 8*, 5−7.
19. Lambe, C. U., and Nelson, D. J. (1982) Pharmacokinetics of inhibition of adenosine deaminase by erythro-9-(2-hydroxy-3-nonyl) adenine in CBA mice, *Biochem. Pharmacol. 31*, 535−539.
20. Agarwal, R. P. (1979) Recovery of 2′-deoxycoformycin inhibited adenosine deaminase of mouse erythrocytes and leukemia L1210 in vivo, *Cancer Res. 39*, 1425−1427.
21. Adachi, H., Takano, M., Yoshimura, Y., Mori, Y., and Sasaki, T. (2002) Promotion of large protein crystal growth with stirring solution, *Jpn. J. Appl. Phys. 41*, L1025−L1027.
22. Niino, A., Adachi, H., Takano, K., Matsumura, H., Kinoshita, T., Warizaya, M., Inoue, T., Mori, Y., and Sasaki, T. (2004) Control of protein crystal nucleation and growth using stirring solution, *Jpn. J. Appl. Phys. 43*, L1442−L1444.
23. Navaza, J. (1993) On the computation of the fast rotation function, *Acta Crystallogr. D49*, 588−591.
24. Bernstein, B. E., Michels, P. A. M., Kim, H., Petra, P. H., and Hol, W. G. J. (1998) The importance of dynamic light scattering in obtaining multiple crystal forms *Trypanosoma brucei* PGK, *Protein Sci. 7*, 504−507.
25. Kinoshita, T., Ataka, M., Warizaya, M., Neya, M., and Fujii, T. (2003) Improving quality and harvest period of protein crystals for structure based drug design: Effects of a gel and a magnetic

field on bovine adenosine deaminase crystals, *Acta Crystallogr. D59*, 1333−1335.
26. Wang, Z., and Quiocho, F. A. (1998) Complexes of adenosine deaminase with two potent inhibitors: X-ray structures in four independent molecules at pH of maximum activity, *Biochemistry 37*, 8314−8324.

BI050529E